

Airflow behavior under different loading schemes and its correspondence to temperature in perishables transported in refrigerated containers

Chanaka Lloyd^{1,2}, Reiner Jedermann¹ and Walter Lang¹

¹ Institute for Microsensors, -actuators and -systems (IMSAS), University of Bremen, Germany. Email: clloyd|rjedermann|wlang@imsas.uni-bremen.de

² International Graduate School for Dynamics in Logistics (IGS), University of Bremen, Germany.

Abstract Supply chains are a highly evolving line of trading. The cool chains responsible for transportation of perishables are one sub category that is demanding technological support to reduce the quality related losses that they suffer due to temperature variations, among other reasons. Even distribution and ventilation of refrigerated air inside containers is imperative to maintain the perishables at the desired temperature range, avoiding degradation and spoilage. However, lack of research on airflow movement behavior—and convenient means of measuring spatial airflow speed—within packed containers makes it difficult to determine the hot spot scenarios, which is a prime cause of the said degradation. This paper presents a methodology to parametrically measure spatial airflow and analyzes the airflow behavior under different container loading schemes and how the airflow affects the internal pallet temperature.

1 Introduction

The preservation of food quality and avoidance of losses in food supply chains is an important target, both at present and in future [Saguy et al. 2013]. Moreover, transportation of perishable food, such as meat, fish, fresh vegetables and fruits, introduces an additional element to the latter challenge: maintaining the desired temperature set point in the refrigerated containers. In consideration of the transportation of, for example, climacteric fruits, supply chains face further challenges in the need to avoid hotspots created by maturing fruits that produce heat [Snowdon 2010]. This paper concentrates mostly on banana transportation. They are transported ideally between 13 and 14 °C. However, even if it is assumed that the

desired temperature is maintained by the cooling unit of the container, bananas could already be at a higher temperature before loading. Therefore, maturation process may have already started which becomes a cascading event and spread throughout a section of the container due to the presence of ethylene, thereby producing heat. This creates isolated hotspots [Moureh et al. 2009]. If the produced ethylene and the warm air are not removed, it causes unwanted degradation of the bananas.

The Intelligent Container project [Lang et al. 2011] and [Grunow and Piramuthu 2013] shows the methods for and importance of the usage of RFID technology in perishable food transportation. In terms of this paper, the focus is on research performed in refrigerated containers packed with bananas. More specifically, the research here is limited to airflow behavior in the refrigerated containers. It helps researchers understand the ventilation process in the container and enables the adoption of correctional measures – changing the banana pallet loading scheme in the container, changing banana box design, increasing the cooling load, etc.

The measurement of airflow within a container is imperative to get a direct measure of the ventilation within a container. However, temperature profiling [Mai et al. 2012 and Jedermann et al. 2010] of a container is the direct measure of the condition of the transported product and is of utmost importance. Therefore, it is highly relevant to correlate airflow and temperature. In measuring the airflow within a container packed with bananas, only the airflow through gaps can be measured. Since measurement of flow (in m^3/h) is not possible, airflow speed (in m/s) is measured at various, spatially distributed locations in real-time using wireless airflow sensors specifically designed for this task.

This paper presents three test cases based on airflow measurements: two comparison tests involving two different banana-pallet loading schemes and a study case on correlation between the airflow around a pallet and its internal temperature. All tests were carried out in a full scale 40-foot container prototype integrated with remote sensing capabilities [Jedermann et al. 2010]. In addition, short section on the wireless airflow sensor is also presented. Apart from few research activities [Laniel et al. 2011 and Ruiz-Garcia et al. 2009], wireless sensors are not heavily used in food transport containers. Therefore, this sensor stands as a good candidate for future research, especially in airflow mapping.

Section 2 illustrates the field test conditions and equipment, airflow sensor (section 2.1), banana loading schemes, and the test cases (section 2.2) mentioned above. Section 3 details the test cases in depth and discusses all the results. Section 4 summarizes and concludes the results.

2 Field tests

The field tests were performed in the container prototype under a scaled down scenario, i.e. using only 11 and 12 banana pallets under two different pallet-

loading schemes. In commercial transportation 20 banana pallets are required to fill a 40-foot refrigerated container. The test cases (section 2.2) presented in this paper compares the two loading schemes for their airflow behavior. Although two cases have different number of pallets, it is the only possibility, as loading/unloading a full scale container of 20 pallets takes long time and effort. Such logistic difficulties prevented the researchers from using a fully loaded container at will.

The aforementioned two loading schemes—*conventional* loading and *chimney* loading—differ only by the way the banana pallets are arranged inside the container. Fig. 1a shows the two loading schemes side by side. It also shows the partition wall, which is raised inside the container right after the last two pallets in order to achieve the scaled down container. Fig. 1b shows a single pallet that is made up of 48 individual banana boxes. The pallet consists of 8 banana box levels, also called *tiers*, called by tier 1, 2, 3...8. Three empty vertical spaces are created in in the chimney scheme, as seen on Fig.1a, due to the loading mechanism.

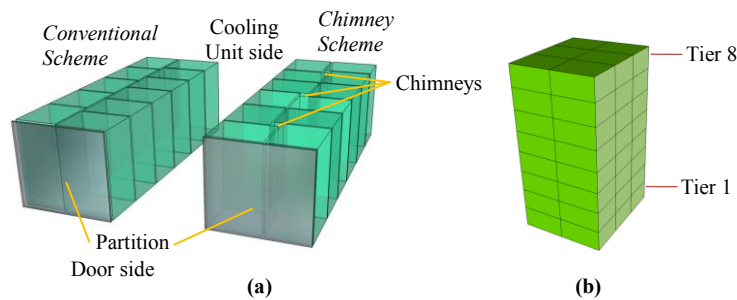


Fig. 1. Banana pallet loading schemes (a); a single banana pallet with 48 banana boxes (b).

The main aim of the field tests was to measure the airflow speed in-between the gaps between adjacent pallets and the spaces between pallets and the container walls, thereby analyze the spatial airflow. In addition, the airflow speed of the input air—pumped in by the cooling unit—in the ducts below the pallets and the return air—absorbed back into the cooling unit—over the pallets were measured. All these types of airflow speed in different gaps describe all major airflow paths in the container. These are depicted in Fig. 2a, which is a cross-section of a banana container as shown in Fig. 1a. The horizontal airflow (input and return air) is not mentioned in this paper but in [Lloyd et al. 2013]. In addition, in order to assess how the airflow affects the temperature inside a banana pallet, two pallets were equipped with 4 temperature sensors and 4 airflow sensors each. This test is further explained in section 2.2.

Fig. 2b shows a pallet affixed with an airflow sensor. The spacers, approx. 1-2 cm thick plastic blocks in place to force a gap—where required—in-between two adjacent pallets, are also shown on either side of the airflow sensor. The sensor is mounted vertically, meaning that it measures the speed of the air that flows from

bottom to top, which is the natural direction for air in a refrigerated banana container [Lloyd et al. 2013]. Most of the tests were conducted using 15 wireless airflow sensors, networked using the BananaHop protocol [Jedermann et al. 2011]. Sensor data was read out in real-time using the remote connection integrated on the intelligent container.

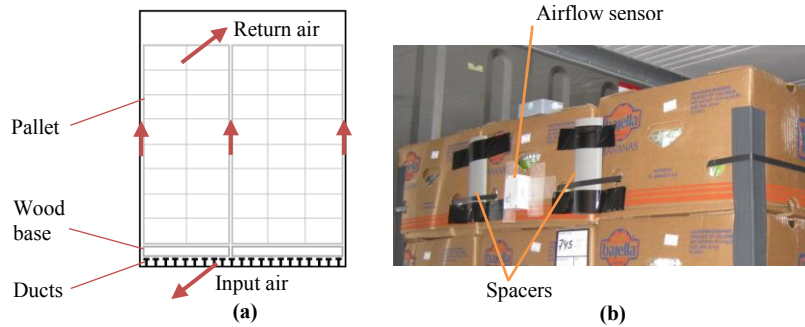


Fig. 2. Cross section of a packed banana container (a); a banana pallet with an airflow sensor and spacers mounted on tier 8 (b).

2.1 Wireless airflow sensor

The airflow sensor is based on a thermal flow sensor [Buchner et al. 2006]. This miniature sensor (Fig. 3) works on the principle of voltage difference between two thermopiles. A heater element in the sensor is powered up and calibrated at 5 mW for the sensors used in the experiments in this paper. This power is maintained throughout the measurement period. The method of sampling the sensor is called the Constant Power (CP) method. The heat dissipation profile of the heater element is disturbed when a flow of air passes over the sensor membrane, which is directly above the heater element. This change is measurable by the difference of the voltage between the two thermopiles. This specially designed airflow sensor [Lloyd et al. 2013], with its circuit, thermal flow sensor and battery, is integrated onto a wireless TelosB platform that is based on IEEE 802.15.4 standard.

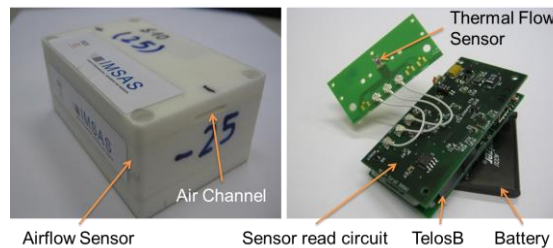


Fig. 3. Wireless airflow sensor enclosure with its air channel (left) and its internal components (right).

2.2 Test cases

The field tests using a packed banana container were conducted in January and May of 2013, with the support of Dole GmbH, Germany. In general, each test was conducted—with the cooling unit running—for approx. 45 minutes. Test case 3 was run for 15 hours. For the purpose of this paper, three test cases are formed:

- **Test case 1**

This is a study of airflow behavior in the gap between the banana pallets and the left container wall along the length of the container from the cooling unit to the partition wall. Airflow movement in this gap for the conventional loading scheme is described in [Lloyd et al. 2013]. This study compares the airflow behavior between the two loading schemes as depicted in Fig. 4a. The airflow sensors were vertically mounted (as in Fig. 2b) on the pallets on tiers 2, 5 and 8. Both the tests—conventional and chimney—were conducted with spacers attached on all aforementioned tiers (also as shown in Fig. 2b), thereby forcing a slight space between the pallets and the container wall along the length of the container.

- **Test case 2**

This test case considers the airflow behavior in the mid-section of the container as shown in Fig. 4b. The spacers were used in this test as well. In conventional setup (left of Fig. 4b), the airflow sensors were mounted only on the tier 8. However, in the chimney setup (right of Fig. 4b) the sensors were mounted on tiers 2, 3 and 8 at the locations indicated on the cross-section figure. Therefore, only the tier 8 sensor values were considered for the comparison of data with the conventional setup.

- **Test case 3**

The main aim of this test (Fig. 5) was to assess how the airflow affects the internal temperature of banana pallets. Therefore, the scenario of a pallet with and without spacers was considered. Ideally, the airflow data around the pallet should be obtained from the same pallet—with and without the spacers—in order to compare the two cases. To implement that, the container needs to be loaded/unloaded two times. The conditions, such as the gaps created when loading the pallets in the second loading, would be different from the first loading. Therefore, in order to monitor the airflow behavior around pallets with/without spacers, two adjacent pallets were chosen, P7 and P8 (P - acronym for Pallet. Pallets are numbered from 1 to 12). P7 was with the spacers around the entire pallet and P8 without. Additionally, temperature sensors, 4 per each pallet, were inserted in the corner boxes on tier 7 of both pallets as

shown in Fig. 5. The test was run for 15 hours from start to finish where the temperature set point of the cooling unit was set to 13 °C (as bananas were pre-cooled to 13 °C), then to 16 °C for 6.5 hours and then back to 13 °C until the sensor batteries died (approx. 6.5 hours).

3 Results

3.1 Test case 1: pallet-wall gap

The setup of test case 1 is shown in Fig. 4a below. A, B, C...F are position identifiers for the sensors that are distributed along the length of the container. At each identifier position, the red square symbolizes three airflow sensors that are placed on 3 different tiers. There were no sensors placed at position identifier D.

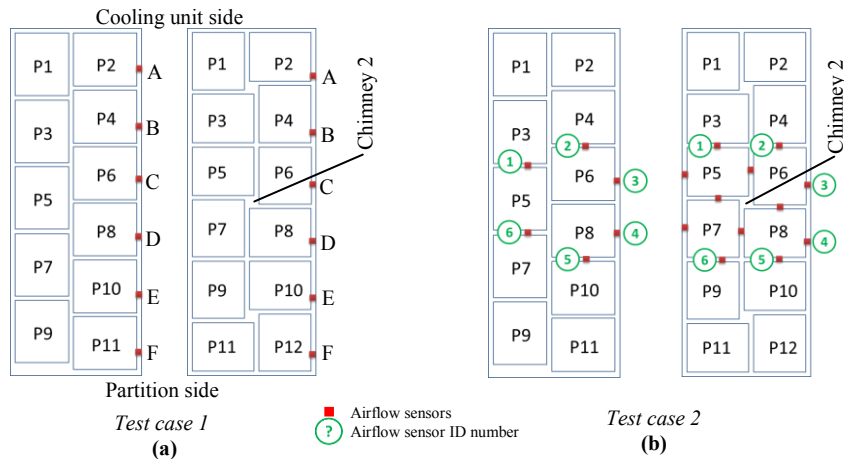


Fig. 4. Airflow sensors in the vertical gap between the pallets and the right-side container wall for both loading schemes (test case 1) (a); airflow sensors in the vertical gaps in-between adjacent pallets in the mid-section of the container under both loading schemes (test case 2) (b).

Table 1 lists the airflow speed values of both the conventional and chimney schemes of test case 1. “-” means there was no sensor there, data unavailable or data is too erroneous. Three chimneys are formed inside the container under this scaled down scenario. All chimneys recorded high airflow speed values than any other vertical airflow speeds in other gaps. For example, chimney 2 airflow speed was approximately 4.5 m/s. The conventional setup does not have any such large,

vertical open shafts. The difference of the different loading schemes is clearly evident when comparing the values in Table 1.

Table 1. Comparison of airflow speed values (at tier 8, 5 and 2 – top to bottom of the pallet) of both the conventional and chimney schemes in test case 1.

Tier	Scheme	A	B	C	E	F
Tier 8	Conventional	0.59	0.60	0.97	1.31	1.18
	<i>Chimney</i>	0.29	0.88	0.27	-	0.83
Tier 5	Conventional	0.35	1.24	0.95	0.61	-
	<i>Chimney</i>	0.55	0.54	1.21	0.28	-
Tier 2	Conventional	0.48	0.99	0.24	0.00	1.09
	<i>Chimney</i>	0.57	-	0.16	0.27	0.20

There are only 4 sensor positions in the chimney setup that exceed the value of the conventional setup by 0.20 m/s or more. In {tier 2, E, conventional} case, it seems the pallet bottom was completely blocking the air flow upwards, hence zero. In all other sensor positions the conventional setup recorded much higher values. Obvious explanation is the presence of the chimneys.

3.2 Test case 2: pallet-pallet gap around container mid-section

The comparison of airflow in the mid-section of the container for both loading schemes is not straight forward. However, the airflow sensors (ID numbers from 1 to 6) shown in Fig. 4b are strategically placed in the conventional scheme in such way that it best resembles the airflow sensor locations of the chimney scheme. Table 2 lists the airflow speed values of both the schemes of test case 2. Again, what is very clear is the vast difference of the airflow behavior between the two loading schemes in the container mid-section as well. With majority of the air escaping at high speed through chimney 2, the values on other vertical gaps around the pallets are far less than that of the conventional case. The airflow values of the 4 vertical gaps that connect to the chimney (values not in Table 2) were even lower, at 0.17, 0.10, 0.28 and 0.52 m/s, which further enforces the theory that air is, in fact, sucked in to the shaft creating a low pressure volume around chimney 2.

Table 2. Comparison of airflow speed values (at tier 8) of both loading schemes in test case 2.

Sensor ID	Conventional scheme (m/s)	Chimney scheme (m/s)
1	1.16	0.33
2	0.82	0.69
3	1.93	0.20

4	-	1.23
5	0.82	0.21
6	2.44	-

3.3 Test case 3: airflow vs. temperature

Test case 3 considers the airflow around two adjacent pallets under the conventional loading scheme, which is how most supply chains transport the banana pallets. The intent of this test was to determine how the airflow around a pallet is different when installed with spacers around it to enable better ventilation, and to assess if such increased ventilation would cause the temperature inside a banana pallet to drop faster. Fig. 5 shows the test setup and how the temperature sensors are inserted in banana boxes.

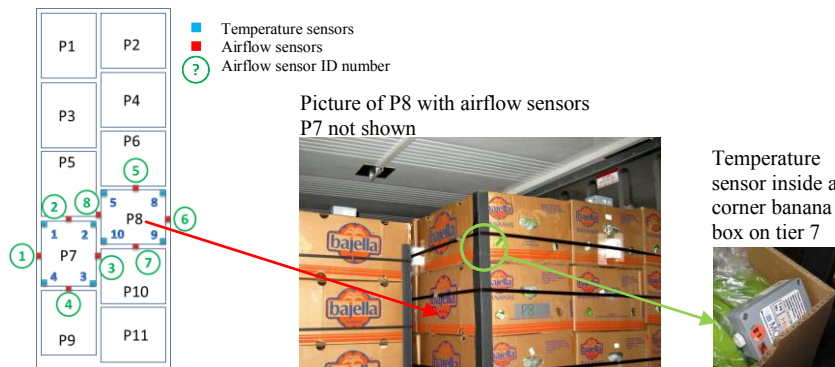


Fig. 5. Test case 3: Airflow sensors in the vertical gaps in-between adjacent pallets and temperature sensors inside corner banana boxes on tier 7, under the conventional scheme. P7 is with spacers and P8 without.

At a single glance of Fig. 6b, which shows the temperature rise (13 to 16 °C) and fall (16 to 13 °C) of all temperature sensors, curves do not coincide or rise together in unison. In order to write off the possibility of sensor error a post-test calibration was run on all 8 sensors (Fig. 6a). It shows how the temperature of all sensors rise together in the red boxes marked on the figure. Temperature offsets were found—maximum being 0.75 °C—and Fig. 6b was compensated accordingly. The temperature sensor numbers (1 to 5 and 8 to 10) are marked in the rectangular boxes in Fig. 6b. An interesting airflow vs. temperature behavior is found when comparing the airflow values of the 8 airflow sensors (1 to 8 in Fig. 5) distributed in the gaps around the two pallets.

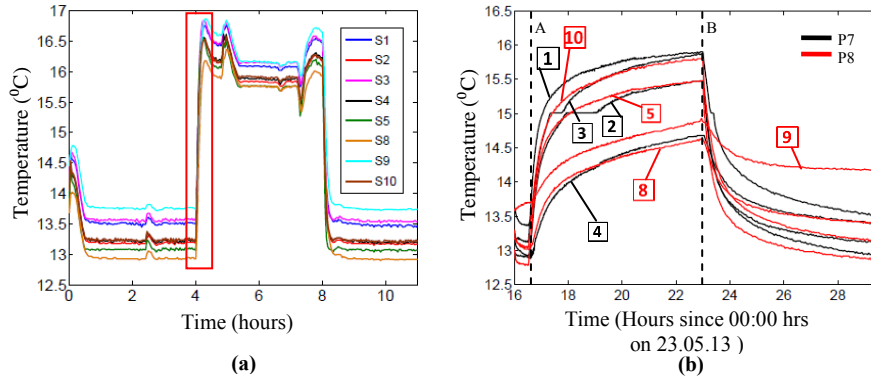


Fig. 6. Calibration of temperature sensors (a); temperature behavior around two pallets with and without spacers (b) over the entire test.

If a tangent line is drawn at the point where the temperature curves meet the dashed line A on Fig. 6b, it is easily discernible that sensor 1, 10, 3, 5 and 2 are having high ascend rates, which indicates that internal temperature of the boxes increased rapidly in comparison to other sensors. The same is true for the cooling cycle beyond dashed line B. The order of descent of temperature was similar to that of the order of ascent. Airflow sensors 1, 2 and 8 recorded values of 1.66, 0.78 and 1.49 m/s. Temperature sensors 1, 2, 5 and 10 are in the neighborhood of these fast airflow paths, which explain the high ascent and descent of temperature. Airflow sensors 3 and 4 recorded values of 0.71 and 0.52 m/s, also much higher compared to other three airflow values on P8 (0.31, 0.69 and 0.47 m/s for airflow sensors 5, 6 and 7, respectively).

Evidently, the airflow values around P7 (with spacers) were much higher than that of P8 (without spacers). Lack of airflow around P8 caused the slow ascent and descent of temperature on temperature sensors 8 and 9, which are sandwiched between the aforementioned three, slow moving drafts around P8. Sensor 4 is special case, where its immediate surroundings are thought to have blocked the airways, hence the slow ascent/descent.

4 Conclusion

Airflow behavior and its effects on pallet temperature were tested. For the purpose of airflow behavior, two banana loading schemes were compared. The chimney scheme clearly exhibits different characteristics to that of the conventional banana loading, where the chimneys funnel most of the upward airflow movement. These comparatively high speed drafts seem to create a low pressure region around the chimney that possibly enhance horizontal airflow movement—towards the chimney shaft—inside the pallets, which is expected to keep the bananas at the desired

temperature during transport. The internal temperature analysis, versus airflow, is not fully deterministic of how the pallet core temperature changes with and without more space around the pallets. However, it shows how the internal contour region located just before the outer surface of the pallet responds to varying airflow speed. These results are encouraging and promising enough to investigate further.

Acknowledgments The research project “The Intelligent Container” was supported by the Federal Ministry of Education and Research, Germany, under the reference number 01IA10001. We thank the support of Dole Fresh Fruit Europe for the provision of test facilities.

References

- Saguy SI, Singh RP, Johnson T, Fryer PJ, Sastry SK (2013) Challenges facing food engineering. *Journal of Food Engineering* 119(2):332-342. doi: 10.1016/j.jfoodeng.2013.05.031
- Snowdon AL (2010) Carriage of bananas (*musa spp.*) in refrigerated ships and containers: preshipment and shipboard factors influencing cargo out-turn condition. *Acta Hort. (ISHS)* 879:375-383. http://www.actahort.org/books/879/879_40.htm
- Moure J, Tapsoba S, Derens E, Flick D (2009) Air velocity characteristics within vented pallets loaded in a refrigerated vehicle with and without air ducts. *International Journal of Refrigeration* 32(2):220-234. doi: 10.1016/j.ijrefrig.2008.06.006
- Lang W, Jedermann R, Mrugala D, Jabbari A, Krieg-Brückner B, Schill K (2011) The Intelligent Container – A Cognitive Sensor Network for Transport Management. *Sensors Journal IEEE* 11(3):688-698. doi: 10.1109/JSEN.2010.2060480
- Grunow M, Piramuthu S (2013) RFID in highly perishable food supply chains – Remaining shelf life to supplant expiry date? *International Journal of Production Economics* 146(2):717-727. doi: 10.1016/j.ijpe.2013.08.028
- Mai NTT, Margeirsson B, Margeirsson S, Bogason SG, Sigurgísladóttir S, Arason S (2012) Temperature mapping of fresh fish supply chains – air and sea transport. *Journal of Food Process Engineering* 35(4):622-656. doi: 10.1111/j.1745-4530.2010.00611.x
- Jedermann R, Moehrke A, Lang W (2010) Supervision of banana transport by the intelligent container. In: Kreyenschmidt J (ed) *CoolChain-Management - 4th International Workshop*. University of Bonn, Germany.
- Laniel M, Émond JP, Altunbas AE (2011) Effects of antenna position on readability of RFID tags in a refrigerated sea container of frozen bread at 433 and 915 MHz. *Transportation Research Part C: Emerging Technologies* 19(6):1071-1077. doi: 10.1016/j.trc.2011.06.008
- Ruiz-Garcia L, Lunadei L, Barreiro P, Robla I (2009) A Review of Wireless Sensor Technologies and Applications in Agriculture and Food Industry: State of the Art and Current Trends. *Sensors* 9(6):4728-4750. doi: 10.3390/s90604728
- Jedermann R, Becker M, Görg C, Lang W (2011) Testing network protocols and signal attenuation in packed food transports. *International Journal of Sensor Networks (IJSNet)* 9(3/4):170-181. doi: 10.1504/IJSNET.2011.040238
- Buchner R, Maiwald M, Sosna C, Schary T, Benecke W, Lang W (2006) Miniaturized thermal flow sensors for rough environments. 19th IEEE International Conference on MEMS. Istanbul 582-585. doi: 10.1109/MEMSYS.2006.1627866
- Lloyd C, Issa S, Lang W, Jedermann R (2013) Empirical airflow pattern determination of refrigerated banana containers using thermal flow sensors. 5th International Workshop on Cool Chain-Management. <http://ccm.ytally.com/index.php?id=176>